A Polarization Independent Microlens using Two Blue-Phase Liquid Crystal Layers with Different Kerr Constant

Yan Li, Yifan Liu and Shin-Tson Wu

College of Optics and Photonics, University of Central Florida, Orlando, USA, 32816

Abstract

We propose a new microlens device structure using two polymer-stabilized blue phase liquid crystal layers whose Kerr constant is largely different. Such a polarization independent microlens has a simple structure and desired parabolic phase profile. Its applications for 2D/3D switchable displays and other photonic devices are emphasized.

1. Introduction

Liquid crystal (LC) adaptive lenses with tunable focal length have various applications such as auto-focusing [1], 2D/3D switchable displays [2,3], and tunable photonic devices [4,5]. Most LC lenses employ nematic LCs because of their high birefringence, simple alignment, and low operation voltage. However, to achieve a short focal length, a relatively thick LC layer (~30 μm) is needed so that the response time is in the order of 1s [6]. Moreover, most nematic LC lenses are polarization dependent. To overcome this problem, two orthogonal devices are stacked together [7].

Recently, polymer-stabilized blue-phase liquid crystal (BPLC) based on Kerr effect [8-10] is emerging as an attractive candidate for photonics applications. It exhibits several major advantages: 1) submillisecond response time [11,12], and 2) alignment free. In 2010, a hole-patterned microlens using polymer-stabilized BPLC was proposed [13]. The device structure is simple, but the phase profile is not exactly parabolic; and the extraordinary and ordinary polarizations have slightly different performances. In 2011, a polarization independent blue phase lens using a curved iridium tin oxide (ITO) electrode was proposed [14], but the fabrication of such structures seems complicated. Another BPLC gradient-index lens with planar multi-electrodes [15] was proposed to realize parabolic phase profile at different focal lengths by addressing the pixelated electrodes individually. In such a structure, electrodes are easier to fabricate while good image quality is maintained. However, an additional high dielectric constant layer is needed to lower the operating voltage and realize polarization insensitivity; moreover, multiple data driving is required. Recently, a BPLC lens with a resistive film [16] have shown attractive performances with single data driving, however, the technology of resistive film on microlenses is not mature yet.

In this paper, we propose a new microlens structure using two PSBP LC layers. The Kerr constant of the first PSBP layer is much larger than that of the second one. Due to the curved interface of the two PSBP layers, optical power is generated. Such a microlens has several attractive features: simple structure, good phase profile, polarization independence, and fast response time. Therefore, it has potential application for 2D/3D switchable displays.

2. Device structure and principle

Figure. 1 depicts the side view of the proposed BPLC lens. Sandwiched between top and bottom planar ITO glass substrates are a convex PSBP-1 layer and a concave PSBP-2 layer. PSBP-1 has a similar dielectric constant and refractive index as PSBP-2, but a much smaller Kerr constant. This can be obtained by using the same LC host and photocurable monomers, but with different pitch lengths. The radius of the lens aperture is R, the central thickness of PSBP-2 is d_1, and the edge thickness is d_2.

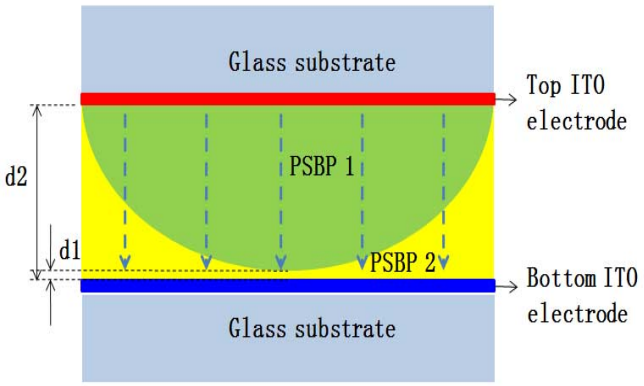

Fig. 1. Side view of the proposed adaptive PSBPLC lens.

When no voltage is applied, there is no optical power because of matched index between the BPLC layers. Once a voltage is applied between top and bottom ITO electrodes, uniform vertical electric fields are generated across the lens due to matched dielectric constant. In PSBP-1, since the Kerr constant is small, the refractive index change is small and the normally incident light sees $n_{ave}=(2n_o+n_e)/3$. In PSBP-2, uniform refractive index change occurs across the lens, following extended Kerr effect [17] $\Delta n_{ind}(E) = \Delta n_s[1-\exp(-(E/E_s)^2]$, where Δn_s is the saturation induced birefringence of the BPLC composite and E_s is the saturation electric field. For normal incidence, light experiences a decreased refractive index $n_o=n_{ave}-\Delta n_{ind}(E)/3$ in PSBP-2. The phase profile at any radius is calculated based on the total optical path lengths in PSBP-1 and PSBP-2. Due to the concave shape and decreased refractive index in PSBP-2 layer, a phase profile like a positive lens is formed.

In our design, because the refractive index change is uniform, the shape of the PSBP-2 layer determines the optical power. We could reduce the operating voltage by optimizing the interface between PSBP-1 and PSBP-2. Moreover, because the electrodes are planar and the dielectric constants of PSBP-1 and PSBP-2 match well, uniform vertical electric fields are generated with very little horizontal components. By suppressing the horizontal components, the device is polarization independent [14].

 ISSN 0097-966X/13/4403-1282-$1.00

3. Material preparation and measurement

We prepared two BPLC mixtures using the same LC host, HTG135200-100 (from HCCH, China) and high twisting power chiral dopant R5011 (from HCCH). The recipes for sample I and sample II are listed in Table 1, where RM257 (Merck) and TMPTA (Sigma Aldrich) are photocurable monomers. The host LC has following physical properties: Δn =0.205 at λ =642 nm, $\Delta\varepsilon$ =85 at 1 kHz and 21 °C. Different amount of R5011 was used to control the pitch length (or Kerr constant) of the two BPLC mixtures.

Table 1. Recipes of the employed BPLC mixtures.

	HTG	R5011	RM257	TMPTA
Sample I	78.0%	10.0%	7.2%	4.8%
Sample II	87.0%	5.0%	4.8%	3.2%

In experiment, we injected the precursors into two vertical field switching (VFS) cells with a 5-μm cell gap [18]. The transition temperature of the precursors between chiral nematic and blue phase during the heating process is 32.7°C for sample I and 68.7°C for sample II. They were cured during cooling process at 33°C and 70°C, respectively, with an UV light (8 mW/cm^2) for 10 min. After the BP mixtures were polymerized, we measured the voltage-dependent transmittance (VT) curves of the two VFS cells using the same method as reported in [18]. The incident angle is 70^o and wavelength is 633nm. Results are shown in Fig. 2.

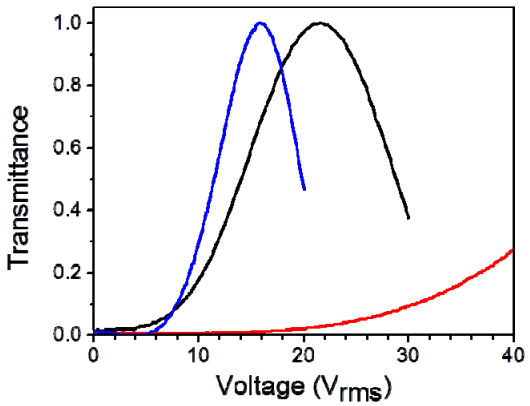

Fig. 2. VT curves of PS-BPLC samples: red curve for sample I, black for sample II and blue for JNC sample.

The red curve represents the VT curve of sample I, and black one represents sample II. We can see that the on-voltage of sample II is much lower than that of sample II, indicating the Kerr constant of sample II is much larger. Because Kerr constant is proportional to the square of pitch length [19], the larger concentration of chiral dopant in sample I results in a shorter pitch length and smaller Kerr constant compared to sample II. After fitting with extended Kerr model, we obtained the saturation birefringence Δn_s=0.18, and saturation electric field E_{s1}= 34.15 V/μm for sample I and E_{s2}=11.1 V/μm for sample II. Also depicted here is the VT curve of a large Kerr-constant JNC PSBP reported in [18] (Δn_{sat}= 0.142 and E_s=4.15 V/μm). By using this large Kerr constant PSBP LC composite, the operating voltage could be greatly reduced. For the simulation using JNC material, we assume that the original JNC PSBP serves in the sample I, and sample II uses a material with the same Δn_{sat} as sample I, but E_s=40 V/μm.

4. Simulation results

After getting the physical properties of samples, we carried out simulation assuming PSBP-1 is the HTG sample I, and PSBP-2 is sample II. First, we used the average dielectric constants of PSBP-1 (ε_{ave1}=25) and PSBP-2 (ε_{ave2}=34) to obtain electric potential distribution using TechWiz. Then we used the extended Kerr model to calculate the induced birefringence in the PSBP layers and the phase profile across the lens. In the simulation, we assume d_1=1 μm, and d_2=12 μm. The radius of the microlens is 180 μm, the total PSBP cell gap is 12 μm and the shape of PSBP-1 is sinusoidal. Figure 1(a) shows the phase profile using HTG samples at 100V$_{rms}$ and λ=633nm.

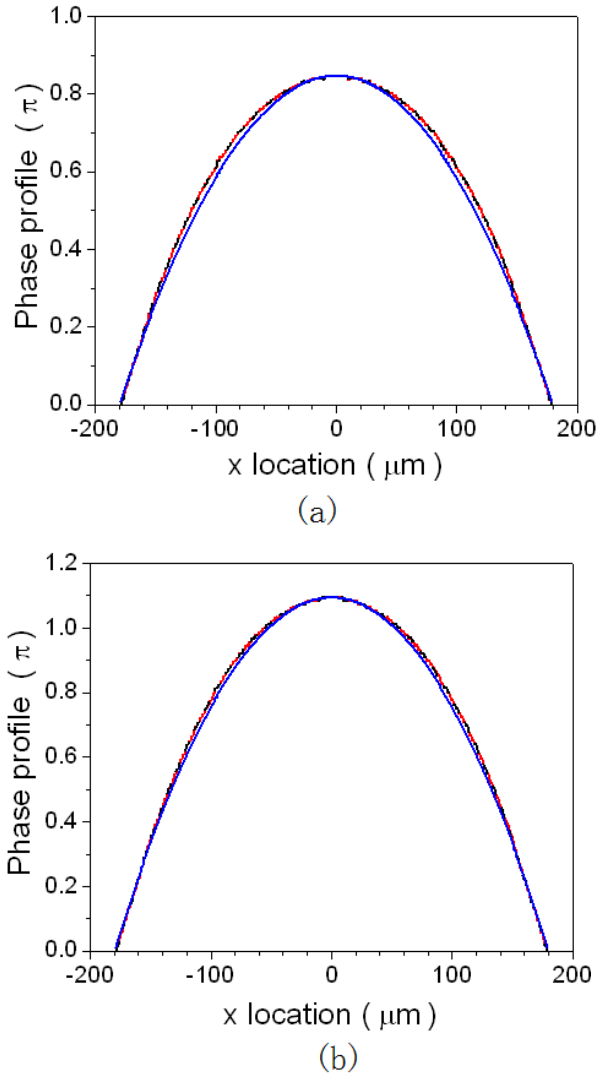

Fig. 3 Phase profiles of proposed adaptive lens: (a) using the HTG samples at 100V$_{rms}$ and (b) using JNC material at 50V$_{rms}$. Red curves are for ordinary (*o*-) wave, black curves are for extraordinary (*e*-) wave, and blue curves are ideal parabolic shapes.

The red (*o*- wave) and black (*e*- wave) curves overlap very well, indicating that the lens is polarization independent. This is due to the close match of the dielectric constant and uniform vertical electric fields generated along the lens. Moreover, both curves match closely to an ideal parabolic shape as depicted by the blue curve, which means aberration would be suppressed. Using the HTG BPLC, we are able to get about 0.9 π phase difference between lens center and edge at $100V_{rms}$. The voltage is still high because the Kerr constants of the samples are relatively small. In Fig. 3(b), we show the phase profile using the large-Kerr-constant JNC material. A larger phase difference 1.1 π phase difference is achieved at a much lower voltage $50V_{rms}$.

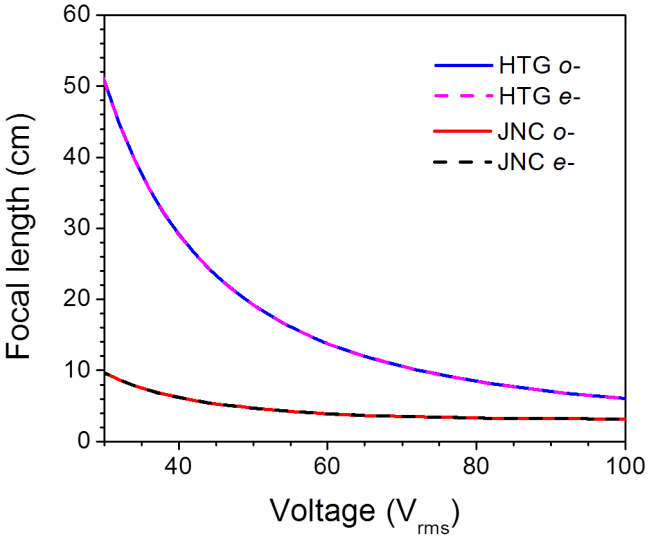

Fig. 4. Simulated voltage-dependent focal length of the proposed BPLC lens.

The focal length at different voltages was calculated using $f = R^2 / 2\Delta\Phi(E)$ where $\Delta\Phi(E)$ is the phase difference between the lens center and edge. As shown in Fig. 4, the blue and pink curves are focal lengths for *o*- and *e*-waves using HTG materials; and the red and black curves are *o*- and *e*-waves using JNC materials. For the JNC material, at around 50Vrms, a focal length of 4cm is obtained.

5. Conclusion

We have proposed a polarization-independent and fast-response microlens using two polymer-stabilized BPLCs. Due to the curved interface and large Kerr constant difference in two PSBP layers, an optical power is generated and can be tuned continuous from infinity to 4cm . Employing the same host liquid crystal, the two PSBP LCs have similar dielectric constant, resulting in vertical electric fields and polarization independence. The use of planar electrodes and single data driving greatly simplify the fabrication complexity. With a simple structure, good phase profile, polarization independence and fast response time, this new microlens has potential applications for 2D/3D switchable displays, naked-eye 3D displays, and active 3D eyeglasses.

6. References

[1] S. Sato, "Liquid-crystal lens-cells with variable focal length," Jpn. J. Appl. Phys. **18**, 1679-1684 (1979).

[2] M. G. H. Hiddink, S.T. de Zwart, O.H. Willemsen and T. Dekker, "Locally switchable 3D displays," SID Symposium Digest, **37**, 1142-1145 (2006).

[3] T. Nose, S. Masuda, S. Sato, J. Li, L. C Chien, and P. J. Bos, "Effect of low polymer content in a liquid crystal microlens," Opt. Lett. **22**, 351-353 (1997).

[4] M. Ferstl and A. Frisch, "Static and dynamic Fresnel zone lenses for optical interconnections," J. Mod. Opt. **43**, 1451-1462 (1996).

[5] P. F. McManamon, T. A. Dorschner, D. L. Corkum, L. J. Friedman, D. S. Hobbs, M. Holz, S. Liberman, H. Q. Nguyen, D. P. Resler, R. C. Sharp, and E. A. Watson, "Optical phased array technology," Proc. IEEE **84**, 268-298 (1996).

[6] H. Ren, D. Fox, B. Wu, and S. T. Wu, "Liquid crystal lens with large focal length tunability and low operating voltage," Opt. Express **15**, 11328-11335 (2007).

[7] Y. H. Lin, H. Ren, Y. H. Wu, Y. Zhao, J. Fang, Z. Ge, and S. T. Wu, "Polarization-independent liquid crystal phase modulators using a thin polymer-separated double-layered structure," Opt. Express **13**, 8746-8752 (2005).

[8] H. Kikuchi, M. Yokota, Y. Hisakado, H. Yang, and T. Kajiyama, "Polymer-stabilized liquid crystal blue phases," Nat. Mater. **1**, 64–68 (2002).

[9] Y. Haseba, H. Kikuchi, T. Nagamura, and T. Kajiyama, "Large electro-optic Kerr effect in nanostructured chiral liquid-crystal composites over a wide temperature range," Adv. Mater. **17**, 2311–2315 (2005).

[10] Z. Ge, S. Gauza, M. Jiao, H. Xianyu, and S. T. Wu, "Electro-optics of polymer-stabilized blue phase liquid crystal displays," Appl. Phys. Lett. **94**, 101104 (2009).

[11] K. M. Chen, S. Gauza, H. Xianyu, and S. T. Wu, "Submillisecond gray-level response time of a polymer-stabilized blue phase liquid crystal," J. Display Technol. **6**, 49–51 (2010).

[12] Y. Chen, J. Yan, J. Sun, S. T. Wu, X. Liang, S. H. Liu, P. J. Hsieh, K. L. Cheng, and J. W. Shiu, "A microsecond-response polymer-stabilized blue phase liquid crystals," Appl. Phys. Lett. **99**, 201105 (2011).

[13] Y. H. Lin, H. S. Chen, H. C. Lin, Y. S. Tsou, H. K. Hsu, and W. Y. Li, "Polarizer-free and fast response microlens arrays using polymer-stabilized blue phase liquid crystals," Appl. Phys. Lett. **96**, 113505 (2010).

[14] Y. Li and S. T. Wu, "Polarization independent adaptive microlens with a blue-phase liquid crystal," Opt. Express **19**, 8045–8050 (2011).

[15] C. T. Lee, Y. Li, H. Y. Lin, and S. T. Wu, "Design of polarization independent multi-electrode GRIN lens with a blue-phase liquid crystal," Opt. Express **19**, 17402–17407 (2011).

[16] Y. Li, Y. Liu, Q. Li, and S. T. Wu, "Polarization independent blue-phase liquid crystal cylindrical lens with a resistive film," Appl. Opt. **51**, 2568–2572 (2012).

[17] J. Yan, H. C. Cheng, S. Gauza, Y. Li, M. Jiao, L. Rao, and S. T. Wu, "Extended Kerr effect of polymer-stabilized blue-phase liquid crystals," Appl. Phys. Lett. **96**, 071105 (2010).

[18] H. C. Cheng, J. Yan, T. Ishinabe, and S. T. Wu, "Vertical field switching for blue-phase liquid crystal devices," Appl. Phys. Lett. **98**, 261102 (2011).

[19] P. R. Gerber, "Electro-optical effects of a small-pitch blue-phase system," Mol. Cryst. Liq. Cryst. **116**, 197–206 (1985).